http://dx.doi.org/10.21172/ijiet.131.10

BEM Model for Coupled Natural Convection and Radiation in a Participating Compressible Grey Fluid

Peter Crnjac[1], Tadej Crnjac[2]
[1,2]*Faculty of Mechanical Engineering, University of Maribor, Smetanovaulica 17, SI-2000 Maribor, Slovenia*

Abstract—The objective of this article is to develop a boundary element numerical model to solve coupled problems involving heat energy diffusion, convection and radiation in a square differentially heated cavity filled with participating grey medium. The P_1approximation is used to solve the radiative transfer equation. The governing Navier-Stokes equations are written in the velocity-vorticity formulation for the kinematics and kinetics of the fluid motion. The approximate numerical solution algorithm is based on boundary element numerical model in its macro-element formulation. The developed algorithm is validated by comparing results of radiative heat transfer with benchmark data. Furthermore, the developed algorithm is tested by simulating natural convection and radiation heat transfer under large temperature differences where compressible flow solution is required.
IndexTerms—Boundary element method, fluid flow, heat transfer, radiation, velocity-vorticity.

I. INTRODUCTION

The combined heat transfer of the radiation and natural convection in the participating (absorbing-emitting-scattering) media is significant in many fields of building and industry, including the boiler, furnace, building thermal comfort and solar reactor. The research on the analysis and numerical solution of heat transfer and fluid flow phenomena where radiative heat exchange has an essential contribution, becomes a key aspect for the employment of computational fluid dynamics simulations as a worthwhile complement to experimental research into industry-related problems. These problems involve the solution of the Navier-Stokes equations and radiative transfer equation (RTE).

Radiative heat transfer plays an important role in the heat transfer in cavities [8], [9], [10],[11], [12], [20].Many investigations dealing with coupling natural convection and the radiation in cavities have been conducted with a transparent medium [18], [20]. Participating gasses with heteropolar diatomic molecules, such as carbon dioxide (CO_2) and water vapour, which emit and absorb thermal radiation, have an important effect on the heat transfer in cavities. However, many real engineering problems involve truly absorbing-emitting gases. In this case, volumetric radiation can significantly affect the temperature field which, in turn, induces changes in the fluid dynamic.

Regarding the coupling of radiation with the double diffusive natural convection, most of the available investigations use the simple assumption of fictitious greymedium. In these works, the fluid was generally regarded as optically thick and the radiative fluxes were calculated by using the Rosseland approximation. Ibrahim et al. [8], Mezrhab et al. [12], and Moufekkir et al. [14] have investigated the coupling phenomena in a gas mixture. They considered a more realistic situation of an absorption coefficient of fluid proportional to the local temperature and concentration of the absorbing species. These studies are still limited to the grey gas assumption.

The objective of this article is to develop a boundary element numerical model (BEM) to solve coupled problems involving heat energy diffusion, convective and radiative heat transfer in a participating fluid [15]. BEM has been previously applied for the solution of heat conduction and coupled heat conduction-convection problems by many authors. The addition of radiation was considered by [2], [3]. However, unlike the previous studies [2], [3] in this study we propose the use of the Grey Gas Model (GGM) [1] for the participating medium.

The developed algorithm is tested by simulating natural convection and radiation heat transfer under large temperature differences where compressible flow solution is required [5], [17]. The impact of radiation on the overall heat transfer is presented using the approach for optical thick fluids, i.e. the P_1 radiative model [6]. In the model, we express the incident radiation at a given position in the radiation field by the nonlinear nonhomogeneous modified Helmholtz equation. Under the Marshak boundary condition, we solve the equation iteratively as a coupled system with the energy equation.

Next, the governing equations are transformed with the use of the velocity-vorticity variables formulation into kinematics and kinetics [2]-[4]. By applying BEM, we transform partial differential equations (PDE) into integral equations [7], [21]. To test the validity and accuracy of the proposed numerical scheme, we study the problem of the overall heat transfer in a closed square cavity filled with a grey participating medium. The velocity and temperature fields together with the total heat transfer are calculated for the Rayleigh numbers in the laminar regime, and the solutions compared to the published standard results [9], [10], [14].

II. GOVERNING EQUATIONS

The present development is focused on the laminar flow of compressible isotropic radiation semi-transparent fluid in solution domain $\mathcal{R} = \Omega \times$ where stands for the two-dimensional plane domain bounded by boundary defined by the outward-pointing unit normal , whilst represents time dimension of the transport phenomenon. The mass, momentum and energy equations are given by the following set of nonlinear equations

$$\frac{\partial v_j}{\partial x_j} = -\frac{1}{\rho}\frac{D\rho}{Dt} = \mathcal{D}\,, \tag{1}$$

$$\rho\frac{Dv_i}{Dt} = -\frac{\partial \tau_{ij}}{\partial x_j} - \frac{\partial p}{\partial x_i} + \rho g_i\,, \tag{2}$$

$$c\frac{DT}{Dt} = -\frac{\partial q_j^D}{\partial x_j} - \frac{\partial q_j^R}{\partial x_j}, \tag{3}$$

in the Cartesian frame x_i, where the field functions of interest are velocity vector field $v_i(r_j, t)$, pressure scalar field $p(r_j, t)$ and the temperature scalar field $T(r_j, t)$, ρ and c denote variable mass density and isobaric specific heat capacity per unit volume, $c = \rho c_p$, $t$is time, g_i is gravitational acceleration vector, $\mathcal{D}$ represents the divergence of the velocity field or the local expansion rate, whilst the vector variables q_j^D and $q_j^R$are heat diffusionand radiation fluxes, respectively. The differential operator $D(\cdot)/Dt$ standsfor the Stokes material derivative.

The conservation equations (2) and (3) contain two molecular diffusive fluxes, i.e. τ_{ij} and q_j^D, representing the diffusion of linear momentum and the heat flux vector, respectively. The Newton linear momentum diffusion constitutive model for compressible viscous shear fluid is considered, such as [3]

$$\tau_{ij} = 2\eta\dot{\varepsilon}_{ij} - \frac{2}{3}\eta\mathcal{D}\delta_{ij}, \tag{4}$$

where η is the dynamic viscosity coefficient. For most heat-transfer problems of practical importance, the simplification known as the Fourier law of heat diffusion is accurate enough, namely

$$q_i^D = -k\frac{\partial T}{\partial x_i}\,, \tag{5}$$

where k is the diffusion thermal heat conductivity.

The governing equation for radiative heat transfer is the radiative transfer equation (RTE) and was discussed previously by Crnjac et. al. [2]-[4]. The RTE is based on an energy balance for radiation passing through a differential volume in a participating medium in local thermodynamic equilibrium (LTE).For the coupling of the radiative heat transport with the fluid dynamics, LTE is assumed and the time dependence of the RTE is neglected [13], [19]. It follows from LTE that the temperature of the fluid and the corresponding radiative temperature in the medium are equal. The solution of the RTE implies a considerable computational cost due to the directional nature of the intensity radiation field. This high computational cost limits detail in the simulation of coupled radiation and convection. Therefore, improvements of the numerical methods and the fundamental analysis of these complex phenomena have motivated interest in the scientific community.

The spectral extinction coefficient of the participating medium $K_\lambda(\vec{r}) = a_\lambda(\vec{r}) + \sigma_{s\lambda}(\vec{r})$is defined as the sum of the spectral absorption coefficient $a_\lambda(\vec{r})$ and the spectral scattering coefficient $\sigma_{s\lambda}(\vec{r})$ [19].In the grey medium with constant a and $K$the P_1 approximation reduces the RTE into a nonlinear nonhomogeneous modified Helmholtz equation [2]-[4]

$$\frac{\partial^2 G}{\partial x_j \partial x_j} - \beta G + b = 0\,, \tag{6}$$

with $\beta = 3aK$ and temperature dependent nonhomogeneous term $b = 4\beta\sigma T^4$. The spectral incident radiation function $G_\lambda(\vec{r})$ describes the total intensity i_λ impinging on a point $\vec{r}$ in the medium from all directions [17]

$$G_\lambda(\vec{r}) = \int_0^{4\pi} i_\lambda(\vec{r},\vec{s})\,d\omega \,. \qquad (7)$$

Note that the spectral incident radiation divided by the speed of light G_λ/c is the spectral radiative energy density at location $\vec{r}$ in the radiation field. The divergence of the radiation flux vector in equation (3) can be expressed as the local radiation source term S^R

$$\frac{\partial q_j^R}{\partial x_j} = -a[G - 4\sigma T^4] = -S^R \,. \qquad (8)$$

If it is assumed that the walls are diffuse grey surfaces, the equation (6) is solved using Marshak boundary condition [2]-[4]

$$-\frac{1}{3K}\frac{\partial G}{\partial n}\bigg|_w = \frac{\varepsilon_w}{2(2-\varepsilon_w)}(4\sigma T_w^4 - G_w)\,, \qquad (9)$$

where ε_w is the emissivity of the wall and the subscript w denotes the value of the indicated variable at the wall.
In this study, the grey gas absorption coefficients for participating gases are correlated by Barlow et al. [1], so the following expression is used to calculate a in units of ($\mathrm{m}^{-1}\cdot\mathrm{ba}^{-1}$)

$$a = c_0 + c_1\left(\frac{1000}{T}\right) + c_2\left(\frac{1000}{T}\right)^2 + c_3\left(\frac{1000}{T}\right)^3 +$$
(10)
$$+c_4\left(\frac{1000}{T}\right)^4 + c_5\left(\frac{1000}{T}\right)^5 .$$

Coefficients c_0, c_1, c_2, c_3, c_4 and c_5 are calculated for different gases as suggested by [1]. These curve fits were generated for temperatures between 300 K and 2500 K and may be very inaccurate outside this range.

III. VELOCITY-VORTICITY FORMULATION OF NAVIER-STOKES EQUATIONS

Substituting equations (4) and (5) for the non-convective heat and momentum fluxes in conservation equations (2) and (3) the following system of nonlinear Navier-Stokes equations for the primitive variables is developed

$$\frac{\partial v_j}{\partial x_j} = -\frac{1}{\rho}\frac{D\rho}{Dt} = \mathcal{D}\,, \qquad (11)$$

$$\rho\frac{Dv_i}{Dt} = -e_{ijk}\frac{\partial \eta\omega_k}{\partial x_j} + 2e_{ijk}\frac{\partial\eta}{\partial x_j}\omega_k + 2\frac{\partial\eta}{\partial x_j}\frac{\partial v_i}{\partial x_j} +$$

$$+\frac{4}{3}\frac{\partial\eta\mathcal{D}}{\partial x_i} - 2\mathcal{D}\frac{\partial\eta}{\partial x_i} - \frac{\partial p}{\partial x_i} + \rho g_i\,, \qquad (12)$$

$$c\frac{DT}{Dt} = \frac{\partial}{\partial x_j}\left(k\frac{\partial T}{\partial x_j}\right) + S^R, \qquad (13)$$

where e_{ijk} is the unit tensor. Representing the transport properties of the fluid as a sum of a constant and variable part, i.e. $\eta = \eta_0 + \tilde{\eta}$, $k = k_0 + \tilde{k}$, $c = c_0 + \tilde{c}$ and $\rho = \rho_0 + \tilde{\rho}$, the momentum and energy equations (12) and (13) can be stated in analogy to the transport equations formulated for the constant transport properties

$$\frac{Dv_i}{Dt} = -e_{ijk}\,\nu_0 \frac{\partial \omega_k}{\partial x_j} - \frac{1}{\rho_0}\frac{\partial p}{\partial x_i} + \frac{\rho}{\rho_0} g_i + \frac{1}{\rho_0} f_i^m \,, \qquad (14)$$

$$\frac{DT}{Dt} = a_0 \frac{\partial^2 T}{\partial x_j \partial x_j} + \frac{S^R}{c_0} + \frac{S_T^m}{c_0} \,, \qquad (15)$$

where the pseudo body force term f_i^m and pseudo heat source term S_T^m are introduced into the momentum equation (12) and into energy equation (13) respectively, capturing the variable transport property effects, and given by expressions

$$f_i^m = -e_{ijk}\frac{\partial \tilde{\eta}\omega_k}{\partial x_j} + 2e_{ijk}\frac{\partial \tilde{\eta}}{\partial x_j}\omega_k + 2\frac{\partial \eta}{\partial x_j}\frac{\partial v_i}{\partial x_j} + \qquad (16)$$

$$+\frac{4}{3}\frac{\partial \eta \mathcal{D}}{\partial x_i} - 2\mathcal{D}\frac{\partial \eta}{\partial x_i} - \tilde{\rho} a_i \,,$$

while the pseudo heat source term is given by an expression

$$S_T^m = \frac{\partial}{\partial x_j}\left(\tilde{k}\frac{\partial T}{\partial x_j}\right) - \tilde{c}\frac{DT}{Dt} \quad (17)$$

in which the kinematic viscosity is $\nu_0 = \eta_0/\rho_0$, the heat diffusivity $a_0 = k_0/c_0$ and the inertia acceleration vector is $\vec{a} = D\vec{v}/Dt$.

In velocity-vorticity formulation the fluid motion computation procedure may be partitioned into its kinetics and kinematics. The kinematics deals with the relationship and restriction among the velocity field at any given instant of time, the vorticity $\omega_i = e_{ijk}\,\partial v_k/\partial x_j$ and local expansion field at the same instant, and given by the following vector elliptic Poisson equation for the velocity vector

$$\frac{\partial^2 v_i}{\partial x_j \partial x_j} + e_{ijk}\frac{\partial \omega_k}{\partial x_j} - \frac{\partial \mathcal{D}}{\partial x_i} = 0 \,. \qquad (18)$$

For the known vorticity and local expansion field functions, the corresponding velocity vector can be determined by solving equation (18), providing that appropriate boundary conditions for the velocity are prescribed, i.e. normal and tangential component of the velocity vector.

The kinetic aspect of the fluid motion is governed by the vorticity transport equation

$$\frac{\partial \omega_i}{\partial t} + \frac{\partial v_j \omega_i}{\partial x_j} = \nu_0 \frac{\partial^2 \omega_i}{\partial x_j \partial x_j} + \frac{\partial \omega_j v_i}{\partial x_j} +$$

$$+\frac{1}{\rho_0} e_{ijk}\frac{\partial \rho g_k}{\partial x_j} + \frac{1}{\rho_0} e_{ijk}\frac{\partial f_k^m}{\partial x_j} \,, \qquad (19)$$

describing the redistribution of the vorticity in the fluid domain by different transport phenomena, e.g. diffusion, convection, twisting and stretching, whilst the buoyancy, compressibility, and the nonlinear terms act as a source or strengthen terms [3].

For the two-dimensional plane motion the equations (18) and (19) significantly reduce to plane kinematics given by the following equation

$$\frac{\partial^2 v_i}{\partial x_j \partial x_j} + e_{ij}\frac{\partial \omega}{\partial x_j} - \frac{\partial \mathcal{D}}{\partial x_i} = 0\,, \qquad (20)$$

whilst the kinetics is expressed by the scalar vorticity equation

$$\frac{\partial \omega}{\partial t} + \frac{\partial v_j \omega}{\partial x_j} = \nu_0 \frac{\partial^2 \omega}{\partial x_j \partial x_j} - \frac{1}{\rho_0} e_{ij}\frac{\partial \rho g_i}{\partial x_j} - \frac{1}{\rho_0} e_{ij}\frac{\partial f_i^m}{\partial x_j}\,. \quad (21)$$

To derive the pressure equation, the divergence of equation (14) should be calculated, resulting in the elliptic Poisson pressure equation [3]

$$\frac{\partial^2 p}{\partial x_i \partial x_i} - \frac{\partial f_{pi}}{\partial x_i} = 0\,, \qquad (22)$$

where in the vector function f_{pi} the diffusion, inertia, gravitational and nonlinear material property effect are incorporated

$$\frac{\partial p}{\partial x_i} = f_{pi} = -\eta_0 e_{ijk}\frac{\partial \omega_k}{\partial x_j} - \rho_0 a_i + \rho g_i + f_i^m\,. \qquad (23)$$

IV. BOUNDARY-DOMAIN INTEGRAL EQUATIONS

In general, the set of equations (6), (20), (21) and (22) have to be transformed, using the Green identities or weighted residual techniques in combination with appropriate fundamental solutions, into boundary-domain integral equations[2]-[4].The singular boundary-domain integral representation for the velocity vector can be formulated rendering the following integral formulation for the two-dimensional plane kinematics

$$c(\xi)v_i(\xi) + \int_\Gamma v_i q^* d\Gamma = e_{ij}\int_\Gamma v_j q_t^* d\Gamma - e_{ij}\int_\Omega \omega q_j^* d\Omega -$$

$$-e_{ij}\int_\Omega \omega q_j^* d\Omega + \int_\Omega \mathcal{D} q_i^* d\Omega\,, \qquad (24)$$

where $u^*(\xi,s)$ stands for the elliptic Laplace fundamental solution

$$u^*(\xi,s) = \frac{1}{2\pi}\ln\left(\frac{1}{r}\right). \qquad (25)$$

In equation (24) we note $q^* = \partial u^*/\partial n$ and $q_t^* = \partial u^*/\partial t$ for the normal and tangential derivative of the fundamental solution, while the quantity $r(\xi,s)$ is the distance vector, which points from the source point ξ to the field point s. The geometrical coefficient $c(\xi)$ denotes the fundamental solution related coefficient depending on the position of the source point ξ.

Considering the kinetics in an integral representation one has to take into account parabolic diffusion character of the vorticity transport equation (21). Applying the linear diffusion differential operator the following boundary-domainintegral representation corresponding to equation (21) can be derived as

$$c(\xi)\omega(\xi,t_F) + \nu_0\int_\Gamma \int_{t_{F-1}}^{t_F} \omega q^* dt\, d\Gamma = \nu_0 \int_\Gamma \int_{t_{F-1}}^{t_F} \frac{\partial \omega}{\partial n} u^* dt d\Gamma$$

$$+\frac{1}{\rho_0}\int_{\Gamma}\int_{t_{F-1}}^{t_F}(-\rho_0 v_n\omega+\rho g_t+f_t^m)\,u^*\,dtd\Gamma+$$
$$+\frac{1}{\rho_0}\int_{\Omega}\int_{t_{F-1}}^{t_F}\left(\rho_0 v_j\omega+\rho e_{ij}g_i+e_{ij}f_i^m\right)q_j^*\,dtd\Omega+ \quad (26)$$
$$+\int_{\Omega}\omega_{F-1}u_{F-1}^*\,d\Omega,$$

where u^* is now parabolic diffusion two-dimensional plane fundamental solution [3]

$$u^*(\xi,t_F;\ s;t)=\frac{1}{4\pi\nu_0\tau}\exp\left[-\frac{r^2}{4\nu_0\tau}\right], \quad (27)$$

where (ξ,t_F) and $(s;t)$ are used for the source and reference space and time field points and $\tau=t_F-t$. Quantities v_n, g_t and f_t^m are the normal velocity component, the tangential component of the gravity and nonlinear source vectors, respectively.
The corresponding integral representation of the pressure equation (22) is given by

$$c(\xi)p(\xi)+\int_{\Gamma}pq^*d\Gamma=\int_{\Omega}f_{pi}u_i^*\,d\Omega, \quad (28)$$

where the vector $\vec{f}_p$ is given by equation (23). For given Neumann boundary conditions, the pressure field p is determine with the solution of integral equation (28) taking into account known velocity and vorticity vector field functions, and transport property values.
The integral representation of the nonlinear heat energy diffusion convection transport equation is derived considering the linear parabolic diffusion differential operator yielding the following integral representation [3]

$$c(\xi)T(\xi,t_F)+a_0\int_{\Gamma}\int_{t_{F-1}}^{t_F}Tq^*dt\,d\Gamma=$$
$$=\frac{1}{c_0}\int_{\Gamma}\int_{t_{F-1}}^{t_F}\left(k\frac{\partial T}{\partial n}-cv_nT\right)u^*\,dtd\Gamma-$$
$$-\frac{1}{c_0}\int_{\Omega}\int_{t_{F-1}}^{t_F}\left(\tilde{k}\frac{\partial T}{\partial x_j}-cv_jT\right)q_j^*\,dtd\Omega+ \quad (29)$$
$$+\frac{1}{c_0}\int_{\Omega}\int_{t_{F-1}}^{t_F}\left(Tv_j\frac{\partial c}{\partial x_j}+cTD-\tilde{c}\frac{\partial T}{\partial t}+S^R\right)u^*\,dtd\Gamma+$$

$$+\int_{\Omega} T_{F-1} u^*_{F-1}\, d\Omega \,.$$

The incident radiation equation (6) is an elliptic modified Helmholtz equation and the corresponding boundary-domain integral representation can be stated as

$$c(\xi)G(\xi) + \int_{\Gamma} G q^* \, d\Gamma = \int_{\Gamma} \frac{\partial G}{\partial n} u^* d\Gamma + \int_{\Omega} 4\beta\sigma T^4 u^* \, d\Omega \,, \tag{30}$$

where u^* is now the modified Helmholtz fundamental solution and given by

$$u^* = \frac{1}{2} K_0\left(\sqrt{\beta} r\right) \text{and} \quad q^* = \frac{d_n}{2\pi r^2} \sqrt{\beta} r K_1\left(\sqrt{\beta} r\right) \,, \qquad (31)$$

whilst K_α is a modified Bessel function of the second kind of order α.

V. DISCRETIZED INTEGRAL EQUATIONS

For the numerical approximate solution of the field functions, the corresponding integral equations are further written in a discretized form in which the integrals over the boundary and domain are approximated by a sum of the integrals over all boundary elements and over all internal cells. Since the implicit set of equations is written simultaneously for all boundary and internal nodes, this procedure results in a fully populated influence and system matrices, resulting in large computing times and memory demands, which is especially true considering the fluid flow characterised by a high Reynolds number value [3].

In order to improve computational efficiency of the computation we employ the macro-element approach [16]. The idea is to use a collocation scheme for integral equations for each domain cell separately and require that the field functions and their normal derivatives must obey the compatibility and equilibrium conditions over the domain cell boundaries. The final system of equations for the entire domain is then obtained by adding the sets of equations for each macro-element, resulting in a sparse system matrix suitable to solve with iterative techniques.

In our case, each macro-element consists of four continuous 3-node quadratic boundary elements with 1-node constant approximation for the normal flux, and a 9-node continuous quadratic internal cell [3]. The quadratic interpolation functions have been used since a good approximation of the boundary values of the velocity gradients ensure an accurate evaluation of the boundary vorticity values, which strongly influence the stability of the numerical method. Linear approximation of field functions over each individual time increment is also considered.

VI. TEST EXAMPLES

Details of the geometry and boundary conditions for the simulation of combined natural convection and radiation heat transferare shown in Fig. 1. In order to check the accuracy of the relevant numerical scheme, a test problem was considered previously analyzed by Lari et al.[9]. It can be observed that the results obtained by Crnjac et al. [3] are in excellent agreement with the previous studies by Lari et al. [9].

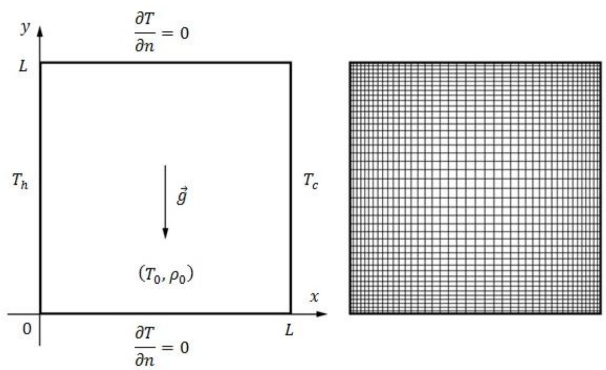

Fig.1.The geometry of the cavity: boundary and initial conditions (left), computational mesh (60x60 cells) (right).

http://dx.doi.org/10.21172/ijiet.131.10

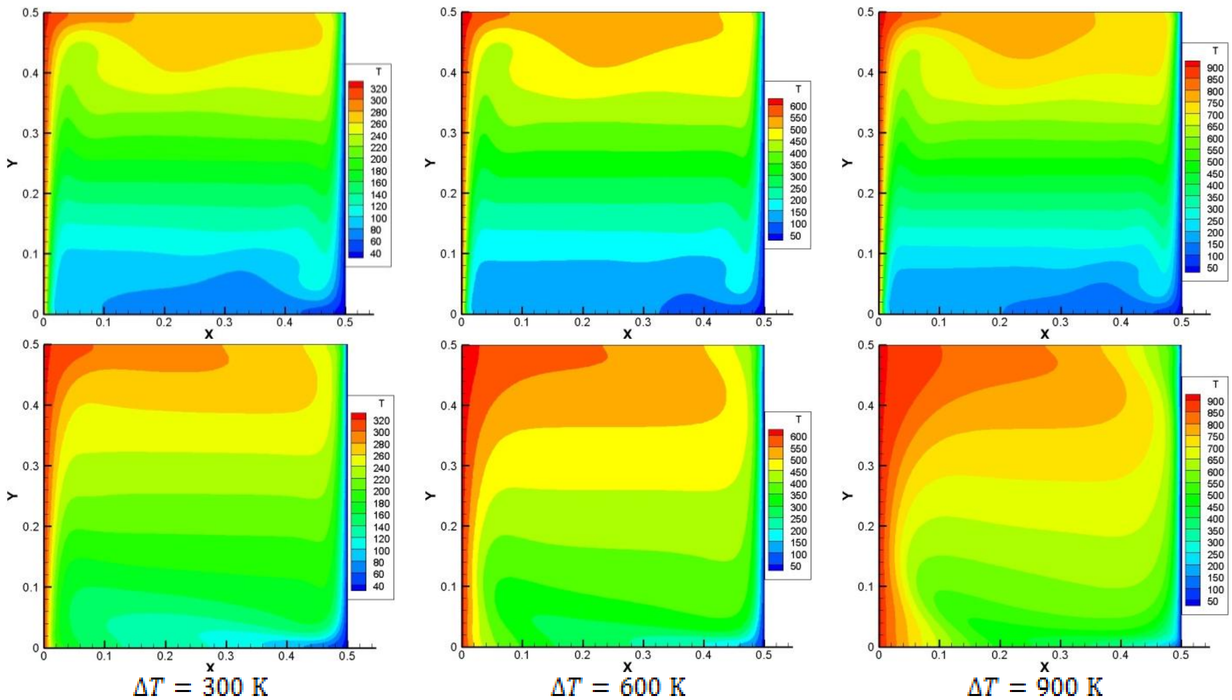

Fig. 2. Temperature fields for different temperature driving potentials, top row: no radiation, bottom row: P_1 model.

The two horizontal walls are perfectly insulated, while the two vertical walls are maintained at two different temperatures T_h and T_c, $(T_h > T_c)$, respectively. The inner surfaces, in contact with the fluid, are assumed to be grey and diffuse. In all test examples we consider a square cavity ($L = 0.5$ m), filled with a Newtonian compressible viscous semi-transparent fluid. It is submitted to a temperature difference $\Delta T = T_h - T_c$ at the vertical walls, with uniform temperatures $T_h = 600$ K, $T_h = 900$ K and $T_h = 1200$ K, respectively, and $T_c = 300$ K. The top and bottom walls of the enclosure are considered adiabatic, i.e. there is no heat flux through them. The initial conditions are given by the value $T_0 = 450$ K and $p_0 = 101{,}325$ Pa. On all walls the no-slip condition is imposed for the velocity. The problem is free of any singularity in the boundary conditions except the presence of the corners in the cavity.

The computational mesh is composed of 240 boundary elements and 3600 internal cells, i.e. 60x60 macro-elements with a ratio of 6 between the longest and the shortest element. The convergence criterion was selected as 10^{-7}. The present time-dependent analyses were performed by running the simulation from the initial state with a time step value of ΔT =1s.

Because the density of the fluid depends on the temperature, the fluid starts moving upward at the hot wall due to buoyancy, and downward at the cold wall. The velocity of the fluid depends on the Rayleigh number

$$Ra = Pr \frac{g \rho_r^2 (T_h - T_c) L^3}{T_r \eta_r^2}, \qquad (32)$$

where Pr is the charasteristic nondimensional Prandtl number, L is the dimension of the square cavity, T_r is a reference temperature defined as $T_r = (T_h + T_c)/2$ and $\rho_r(T_r, p_r)$ is a reference mass density.

As a test example, the impact of radiation on the overall heat transfer is analysed by applying the P_1 radiative model. In engineering radiative transfer problems, the P_1 model should typically be used for spectral optical thicknesses $\kappa_\lambda(\vec{r}) = \int_0^S K_\lambda(\vec{r}) dr > 1$[19]. To consider the effect of differing driving forces for buoyant flow, we vary the temperature of the hot wall as the primary variable in this study. As a first numerical example, the impact of radiation on the overall heat transfer is analysed with temperature difference $\Delta T = 300$ K ($Ra = 6.0 \cdot 10^6$). The second computations were performed for $Ra = 3.5 \cdot 10^6$, as a result of imposed $T_h = 900$ K and $T_c = 300$ K. The third example is analysed with temperature difference $\Delta T = 900$ K ($Ra = 2.0 \cdot 10^6$). It was assumed, that the transient simulation results achieved steady state when the selected convergence criteria between two-time steps was satisfied. Let us present the temperature and velocity fields, respectively, predicted by the P_1 model for the case of conduction, radiation and significant levels of convection. Fig. 2 compares the influence of the internal radiation with $\kappa_L = 10$ on the fluid structure for three temperature differences.It is obvious that the radiation transfer is characteristically different from the convection heat transfer and depends on the properties of the medium including the optical thickness. The effects are visible along the horizontal walls and at the core of the cavity. Compared to the case without radiation, fluid circulation is increased under radiation, and isotherms structures in the cavity are affected by thermal radiation.

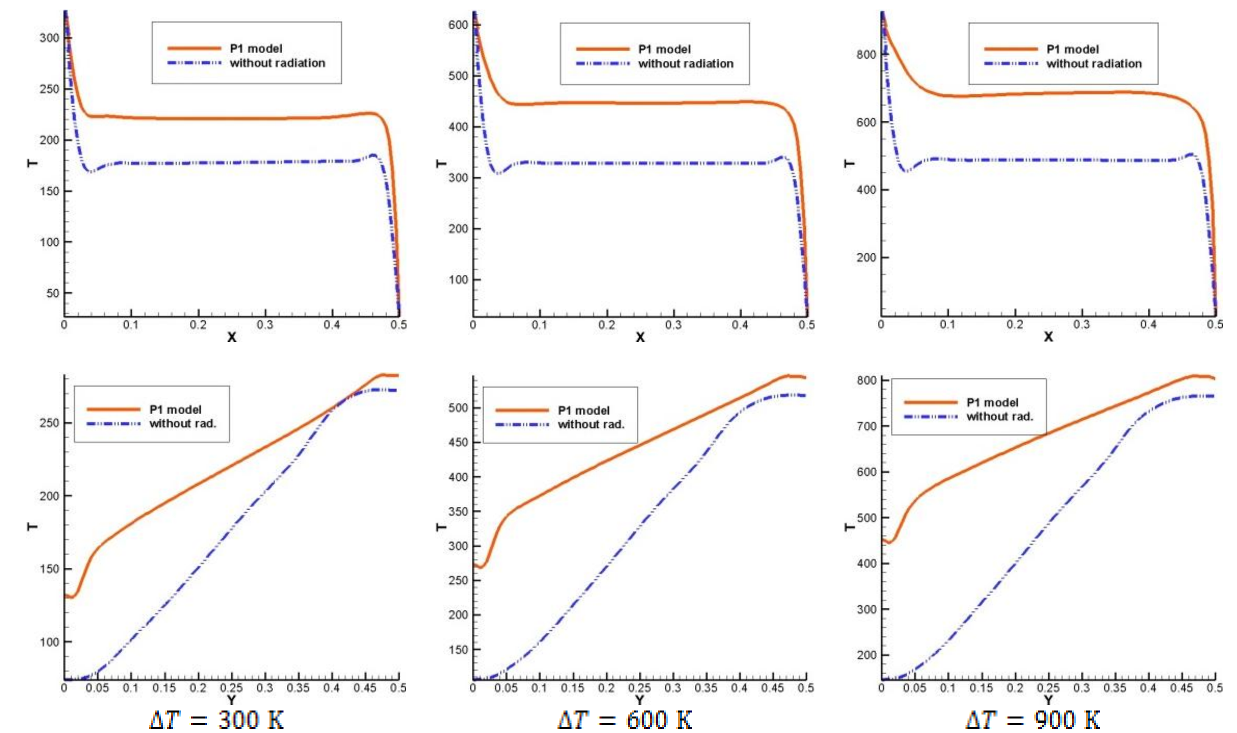

Fig. 3. Horizontal temperature profiles at $y = L/2$ (top row) and vertical temperature profiles at $x = L/2$ (bottom row), solid line:P_1model, dashed line: without radiation.

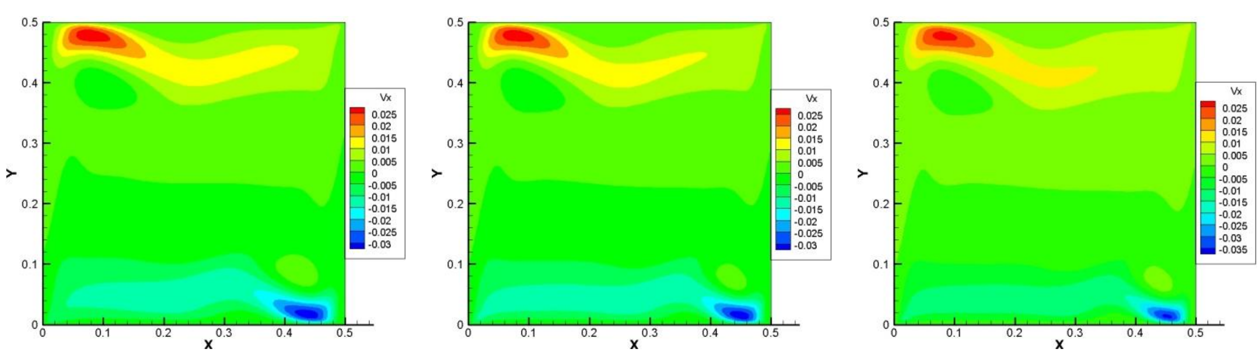

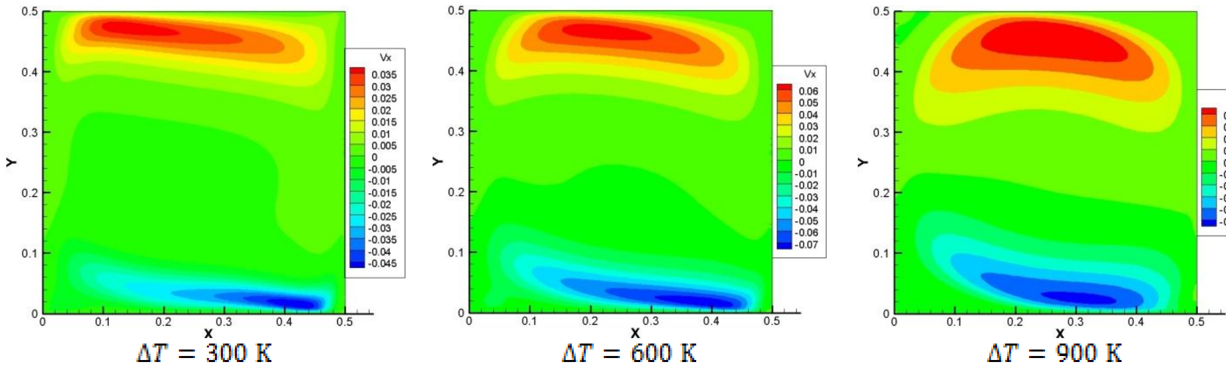

Fig. 4. Horizontal v_x velocity component contours ($\kappa_L = 10$) for different temperature driving potentials; top row: no radiation, bottom row: P_1 model

The differences between both cases are clearer in Fig. 3, where the temperature distributions along the x-axis at $y = L/2$ and along the y-axis at $x = L/2$ are plotted and compared for the same temperature driving potentials. The temperature field predicted with the P_1 model is very similar to the benchmark problem studied by Moufekkir et al. [14]. The temperature field of the P_1 model through the middle portion of the domain is vertically stratified, with nearly horizontal isotherms, and thermal boundary layers have formed along the walls. It appears from the isotherms that the radiation heat transfer produces a good homogenization of temperature.

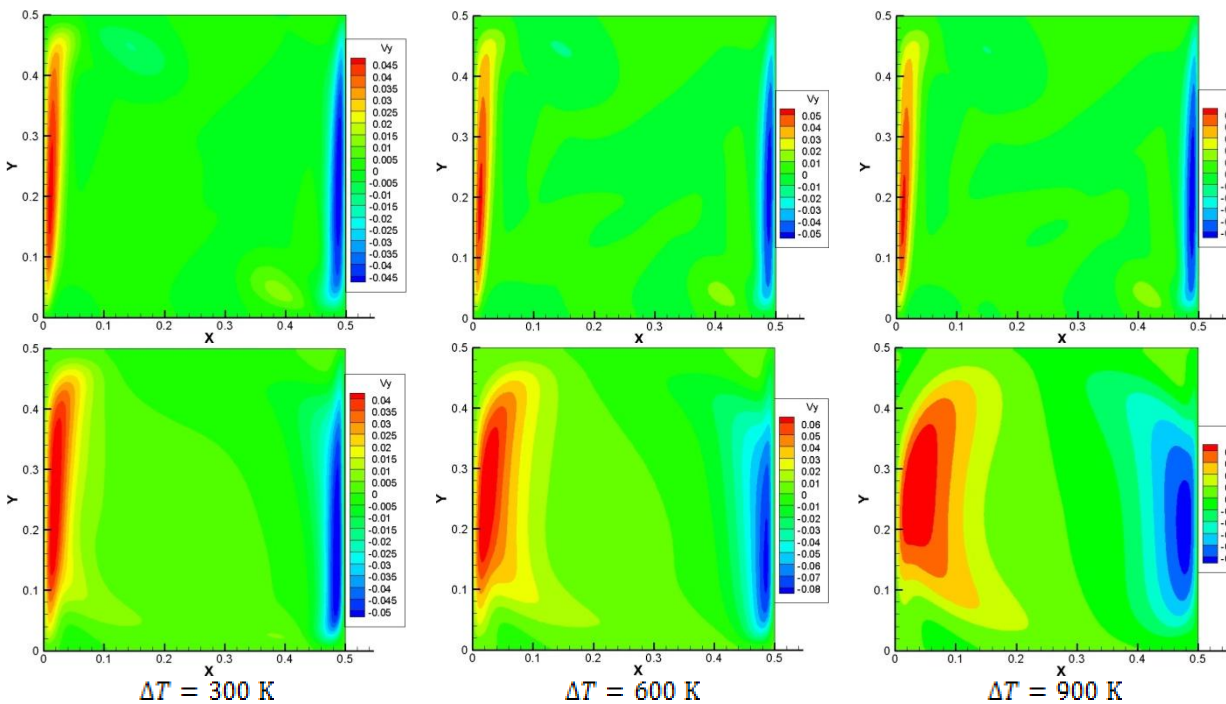

Fig. 5. Vertical v_y velocity component contours ($\kappa_L = 10$) for different temperature driving potentials; top row: no radiation, bottom row: P_1 model

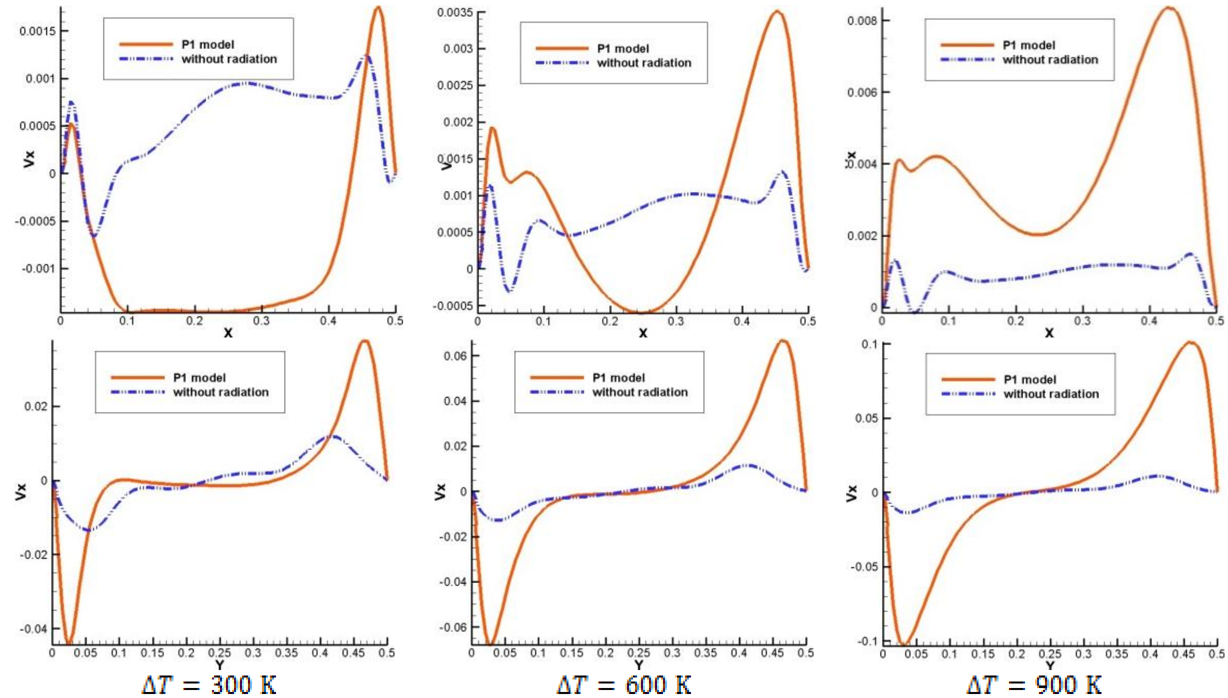

Fig. 6.Horizontal velocity component profiles $v_x(x, L/2)$ along x-axis at $y = L/2$ (top row) and $v_x(L/2, y)$ along y-axis at $x = L/2$ (bottom row) for different temperature driving potentials.

Figs. 4 and 5 show velocity fields for the same temperature driving potentials. The effects of the temperature difference ΔT on horizontal velocity component profiles $v_x\left(x, \frac{L}{2}\right)$ along x-axis at $y = \frac{L}{2}$ and $v_x\left(\frac{L}{2}, y\right)$ along y-axis at $x = L/2$ are shown in Figure 6. Vertical velocity component profiles $v_y(x, L/2$ along x-axis at $y = L/2$ and $v_y(L/2, y)$ along y-axis at $x = L/2$ for different temperature driving potentials are shown in Figure 7

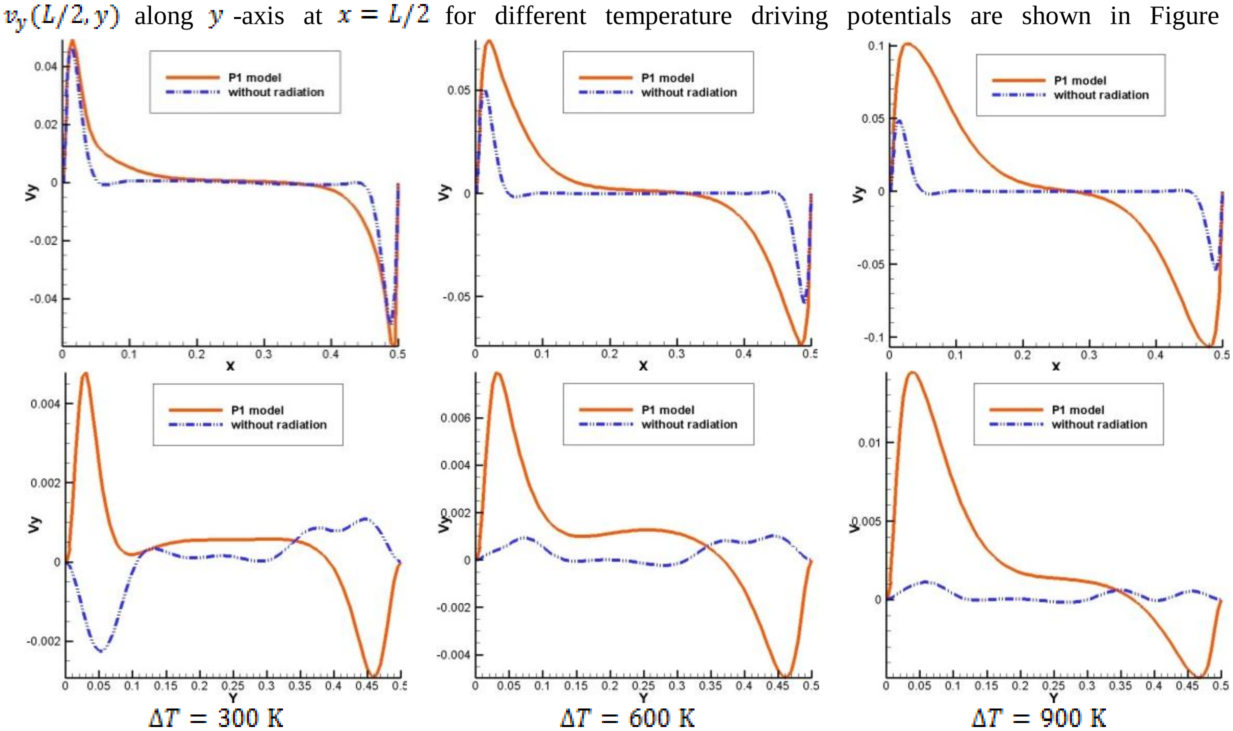

Fig. 7.Vertical velocity component profiles $v_y(x, L/2$ along x-axis at $y = L/2$ (top row) and $v_y(L/2, y)$ along y-axis at $x = L/2$ (bottom row) for different temperature driving potentials.

It is seen that the maximum of both distributions gradually increases with the temperature difference. Indeed, due to increasing ΔT the heat transferring in the cavity increases and hence the driven buoyancy force increases. Thus, higher velocities are acquired. It is also seen in figures that the difference between the velocity profile for the P_1 model and for the pure convection model at each ΔT is considerable.

It was found previously that when Ra increases, the natural convection has the great effects on the temperature distribution and heat transfer in the cavity. The diffusion, radiative and overall Nusselt number at the walls are calculated from the heat fluxes as

$$Nu(y) = \frac{L(q^D + q^R)}{k_r(T_h - T_c)} = Nu_D(y) + Nu_R(y)\,, \qquad (33)$$

$$Nu_D(y) = \frac{L}{k_r(T_h - T_c)} k^D(T) \left(-\frac{\partial T}{\partial x}\bigg|_w \right), \qquad (34)$$

$$Nu_R(y) = \frac{L q_w^R}{k_r(T_h - T_c)}\,, \qquad (35)$$

where$k(T)$ is temperature dependent heat conductivity and $k_r = k(T_r)$. The temperature dependence of the dynamic viscosity is given by the Sutherland model [2] and the heat conductivity is expressed as $k^D(T) = \eta(T)\, c_p / Pr$.

Table 1 shows computed diffusion and radiation Nusselt number values, $Nu_D$and Nu_R, for the hot and cold wall as a function of temperature difference for the mesh M = 60 × 60. We can observe that the Nusselt number Nu_R is in the range of ≈ 135−580 for the hot and ≈ 82−393 for the cold wall, while the Nusselt number Nu_D is in the range of ≈ 10−14 for the hot and ≈ 13−24 for the cold wall. Therefore, $Nu_R = Nu - Nu_D$ is much higher than $Nu_D$for all cases, which indicates that the radiation heat transfer is dominant heat transfer mechanism in the closed cavity.

Tablei: Diffusion And Radiation Nusselt Number Values For The Hot And Cold Wall As A Function Of Temperature Difference

ΔT	P_1 model						without radiation					
	hot wall			cold wall			hot wall			cold wall		
	Nu_D	Nu_R	Nu	Nu_D	Nu_R	Nu	Nu_D	Nu_R	Nu	Nu_D	Nu_R	Nu
300	10.384	135.769	146.153	15.688	82.631	98.319	14.332	-	14.332	14.346	-	14.346
600	10.192	323.032	333.224	17.956	187.340	205.296	14.283	-	14.283	14.243	-	14.243
900	10.054	579.397	589.451	23.499	393.192	416.691	13,811	-	13.811	13.677	-	13.677

VII. CONCLUSION

In this paper we have implemented P_1 approximation to simulate combined problems involving conductive, convective and radiative heat transfer in a 2D square cavity filled with a viscous compressible grey fluid. For the P_1 model the RTE is a diffusion equation, which is easy to solve with little CPU (Central Processing Unit) demand. The P_1model should typically be used for cases with optical thicknesses larger then one. It should be aware of the following limitations when using the P_1 model: P_1 model assumes that all surfaces are diffuse. The implementation assumes grey radiation. There may be a loss of accuracy, depending on the complexity of the geometry, if the optical thickness is small.

The main advantage of boundary-element based simulation algorithms is in the fact that a part of the solution of the underlying problem (the fundamental solution) is used to set up the integral formulation of the problem. This enables higher accuracy of the solution of the problem compared to standard techniques such as finite elements or control volume. This is especially true for diffusion or advection-diffusion type problems, which are considered and which feature high gradients in the solution.

In this paper, we consider optical thickness 10, and discover that at this value the model yielded surprisingly accurate values compared to the published benchmark results. The governing equations of combined heat transfer were solved simultaneously to obtain the temperature and velocity profiles inside the participating medium.However, the model matches very well with the method of discrete ordinates used by Lari et al. [9] to model the radiative heat transfer in optical thick media.Based on the results of this analysis, we recommend the use of the formulation for the buoyant flows in optically thick fluids.

VIII. REFERENCES

[1] R. S.Barlow, A. N.Karpatis, and J. H. Frank,"Scalar Profiles and NO Formation in Laminar Opposed-Flow Partially Premixed Methane/Air Flames,"*Combustion and Flame*, vol. 127, pp. 2102−2118, 2001.

[2] P. Crnjac,L. Škerget, J. Ravnik, and M. Hriberšek, "Implementation of the Rosseland and the P1 radiation models in the system of Navier-Stoke's equations with the boundary element method," *Int. J. of Comp. Meth. and Exp. Meas*., vol. 5, no. 3, pp. 348−358, 2017.

[3] P. Crnjac, L. Škerget, J. Ravnik, and M. Hriberšek, "BEM model for radiative transport phenomena in optically thick compressible viscous fluids," *Engineering Analysis with Boundary Element*, 96 (2018) 1–13.

[4] P. Crnjac, L. Škerget, and J. Ravnik,"The impact of a gas radiation on incompressible fluid flows with the boundary element method," *Tehničkivjesnik,* to be published.

[5] B. Dubroca, M. Seaid, andI. Teleaga, "A consistent approach for the coupling of radiation and hydrodynamics at low Mach number," *Journal of Computational Physics*, vol. 225, no. 1, pp. 1039−1065, 2007.

[6] F. Göbel andC. Mundt, "Implementation of the P1 Radiation Model in the CFD solver NSMB and Investigation of Radiative Heat Transfer in the SSME Main Combustion Chamber," 17th AIAA International Space Planes and Hypersonic Systems and Technologies Conference, San Francisco, California, 11−14 April 2011.

[7] M. Hriberšek and L. Škerget, "Iterative methods in solving Navier-Stokes equations by the boundary element method," *Int. J. Numer. Meth. Eng.*,vol. 39, pp. 115−139, 1996.

[8] A. Ibrahim andD. Lemonnier, "Numerical study of coupled double-diffusive natural convection and radiation in a square cavity filled with a N2-CO2 mixture," *International Communications in Heat and Mass Transfer*, vol. 36, no. 3, pp. 197−202, 2009.

[9] K. Lari,M. Baneshi, S. A. GandjalikhanNassab,A. Komiya, and S. Maruyama, "Combined heat transfer of radiation and natural convection in square cavity containing participating gases," *International Journal of Heat and Mass Transfer*, vol. 54, no. 23−24, pp. 5087−5099, 2011.

[10] V. Le Dez and H. Sadat, "Radiative heat transfer in a semi-transparent medium enclosed in a two-dimensional square cavity," *Journal of Quantitative Spectroscopy and Radiative Transfer*, vol. 112, no. 5, pp. 847−863, 2011.

[11] X. L. Liu,G. C. Gong,and H.S. Cheng, "Combined Natural Convection and Radiation Heat Transfer of Various Absorbing-Emitting-Scattering Media in a Square Cavity," *Advances in Mechanical Engineering*, vol. 6, January-December 2014.

[12] A. Mezrhab, D. Lemonnier, S. Meftah, and A. Benbrik, "Numerical study of double-diffusion convection coupled to radiation in a square cavity filled with a participating grey gas," *Journal of Physics D: Applied Physics*, vol. 41, no. 19, Article ID 195501, 2008.

[13] M. F. Modest, "Radiative Heat Transfer," Third Edition ed., Academic Press, 2013.

[14] F. Moufekkir,M. Moussaoui, A. Mezrhab,M. Bouzidi,and D. Lemonnier, "Combined double-diffusive convection and radiation in a square enclosure filled with semi-transparent fluid," *Computers and Fluids*, vol. 69, pp. 172−178, 2012.

[15] A. Y. Raghu Kumar, "Boundary Element Methods for Thermal Problems-Review," *Int. Journal of Engineering Research & Technology*, vol. 2, no. 10, pp. 2486−2496, 2013.

[16] M. Ramšak and L. Škerget, "A subdomain boundary element method for high-Reynolds laminar flow using stream function-vorticity formulation," *Int. J. Numer. Meth*, vol. 46, pp. 815−847, 2004.

[17] M. Seaid, A. Klar,and R. Pinnau, "Numerical Solvers for Radiation and Conduction in High Temperature Gas Flows," *Journal of Flow Turbulence and Combustion*, vol. 75, pp. 173−190, 2005.

[18] S. Saravanan and C. Sivaraj, "Coupled thermal radiation and natural convection heat transfer in a cavity with a heated plate inside," *International Journal of Heat and Fluid Flow*, vol. 40, pp. 54−64, 2013.

[19] R. Siegel and J. R. Howell, "Thermal radiation heat transfer-4 th ed.," Taylor and Francis, New York, London, 2002.

[20] H. Sun, E. Chénier, and G. Lauriat, "Effect of surface radiation on the breakdown of steady natural convection flows in a square air-filled cavity containing a centered inner body," *Applied Thermal Engineering*, vol. 31, no. 6−7, pp. 1252−1262, 2011.

[21] L. Škerget, M. Hriberšek, and G. Kuhn, "Computational Fluid Dynamics by Boundary Domain Integral Method," *Int. Journal for Numerical Methods in Engineering*, vol. 46, pp. 1291−1311, 1999.

[22] L. Škerget and N. Samec, "BEM for the two-dimensional plane compressible fluid dynamics," *Eng. Anal. Bound. Elem*., vol.29, pp. 41−57, 2005.